ELSEVIER

Journal of Neuroscience Methods 152 (2006) 18–31

JOURNAL OF NEUROSCIENCE METHODS

www.elsevier.com/locate/jneumeth

Quantification of the drawing of an Archimedes spiral through the analysis of its digitized picture

F. Miralles [a,*], S. Tarongí [a], A. Espino [b]

[a] *Gabinet d'Electromiografia Central i Control Motor, Servei de Neurologia, Hospital Universitari Son Dureta, C/. Andrea Doria 55, 07014 Palma de Mallorca, Spain*

[b] *Unitat de Neurologia, Fundació Hospital Son Llatzer, Palma de Mallorca, Spain*

Received 23 April 2005; received in revised form 30 July 2005; accepted 8 August 2005

Abstract

We have developed a new quantitative analysis of spiral drawing that is able to evaluate any spiral execution and it has not temporal or spatial limitations in the obtaining of specimens. Thirty-one patients with action tremor and 24 control subjects were asked to draw an Archimedes spiral over a print template. Specimens were scanned and then treated through a semiautomatic computer program that reconstructs the temporal sequence of the spiral drawing by the subject. The spirals were first analysed by means of the cross-correlation coefficient with the spiral template. Secondly, the mean and the standard deviation of the distance between each point of the spiral drawing and the corresponding point of the spiral model were determined. Finally, the reconstructed spiral was analysed using the Fourier Transform. Its results were interpreted with the aid of a computer model of a tremulous spiral. The experimental variables were greater in the patients group respect to age-matched controls. There was also a high linear correlation between them and the clinical score given by three neurologists. Finally, Receiver Operating Characteristic (ROC) curves analysis shown that the method classified the spirals better than human ratters.

Keywords: Tremor; Motor control; Drawing; Mathematical modelling; Fourier analysis

1. Introduction

The drawing of an Archimedes spiral (spirography) is commonly used in the evaluation of patients with pathologic tremors and other movement disorders. In this respect, spirography has proved to be a valid and convenient measure of the disability caused by postural tremors (Bain et al., 1993). Nevertheless, in most studies spirals are subjectively rated using clinical scales. The availability of an objective procedure of analysis would improve the sensibility and reproducibility of spirography as a method for tremor evaluation. Elble et al. (1990, 1996) were the first who used a digitizing tablet in order to quantify the amplitude and frequency of tremor during handwriting and drawing of a spiral. Their method was designed with the aim to obtain the same type of information as accelerometry but with a lesser cost. Thus, their analysis of the digitized drawings was centred on the amplitude and area of the spectral peak when present. Patients with either no peak in the spectrum or with very severe tremor that caused artifactual discontinuities in data sampling could not be analysed. Subsequently, Pullman (1998) combined the Fourier analysis of the spiral data recorded on a digitizing tablet with other kinematics measures of spiral drawing in order to quantify motor dysfunction of patients with tremor and other movement disorders. However, the description of his method was so schematic that it seems difficult to think that his technique may be of general use. Longstaff et al. (2003) studied the ability of Parkinson's disease patients to draw spirals using also a graphics tablet. These authors quantified the spirals through the r^2 value of the linear regression line determined after the conversion of the raw position data of the digitized spiral into polar co-ordinates – that is, radius and angle of revolution – (see Section 2). Nevertheless, this method is not suitable to analyse patients with tremor because tremors of different amplitude but that oscillate symmetrically around the spiral line would have the same r^2 value. Finally, Liu et al. (2005) quantified the digitized spirals drawn by Parkinson's disease patients with drug-induced dyskinesias by means of the standard deviation of the drawing velocity computed after filtering the raw data in order to

* Corresponding author. Tel.: +34 971175167; fax: +34 971175500.
E-mail address: med013180@nacom.es (F. Miralles).

0165-0270/$ – see front matter © 2005 Elsevier B.V. All rights reserved.
doi:10.1016/j.jneumeth.2005.08.007

subtract the co-existing voluntary drawing movements and action tremor. Thus, its analytical method was designed with the aim to exclude expressly the arm tremor from the spiral quantification.

All the above-descripted objective methods of spiral drawing quantification make use of a digital graphic tablet. This implies that the technical equipment (i.e. a digitizing tablet connected to a personal computer) is needed not only to carry out the mathematical analysis but also to obtain the spiral specimens. Thus, these methods are likely to be only applicable in a hospital, with the artefactual increase in tremor amplitude due to the anxiety, which often accompanies hospital attendance, and with the logical limitations in the number of explorations that can be carried out in a patient.

With the aim to overcome the drawbacks of the presently available methods, we have developed a new procedure of quantification of the drawing of an Archimedean spiral based in the off-line analysis of its digitized picture obtained with a commercial scanner. The present method allows to obtain the patient's spiral specimen without being limited to a determined physical space, even making possible the self-administration of the test in the own patient's home.

2. Materials and methods

The methodology of analysis is summarised diagrammatically in Fig. 1A. It is composed by two different parts. One is the progressive (step-by-step) reconstruction of the spiral as it was drawn by the subject from its digitized picture. The other is the different type of mathematical analysis performed at each stage of the reconstruction (Fig. 1A).

2.1. Execution of the spiral

Patients and controls were asked to overdraw a spiral template with a red pen, printed in black on a paper with their dominant arm. The subjects were seated and the drawings were made without allowing the forearm to rest on the drawing board. Although the drawing was traced at a self-paced velocity, the subjects were encouraged not to stop drawing until completing the spiral. The form and dimensions of the model spiral are show in Fig. 1B.

2.2. Reconstruction of the spiral

Spiral specimens were digitalized at a resolution of 650 × 650 pixels and the images were salved to a 24-bits bitmap file. Then, bitmap files were decodified and displayed in an 8-bits graphic screen. Pixels that represented the spiral drawn by the subject were selected thanks to its different colours (red versus black—colour of the print template or white—background colour) and their x, y co-ordinates were saved to an ASCII file. The origin of the co-ordinates axis (0, 0) was the centre of the model spiral. The spiral was then reconstructed (i.e. x, y spiral pixels co-ordinates were ordained following the temporal sequence in which they were drawn by the subject) through a semi-automatic procedure. With this object, pixels were firstly

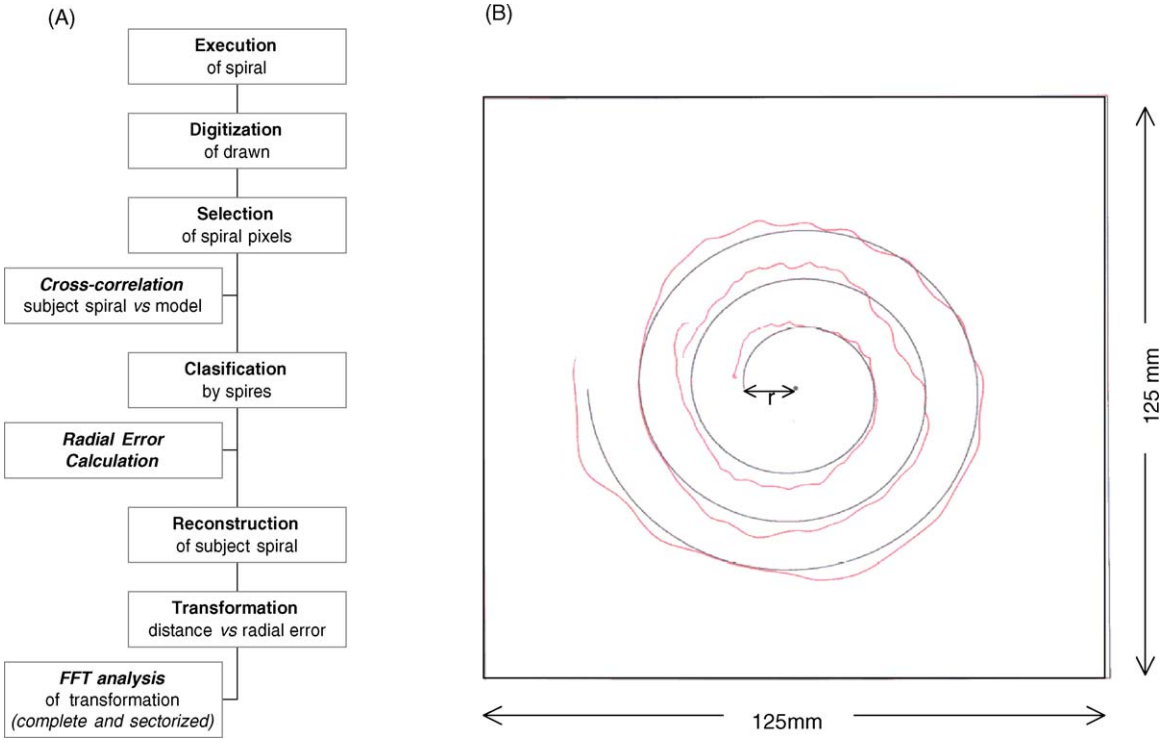

Fig. 1. (A) Diagram of the different steps of the method. The figure shows the two parts of the procedure: the progressive reconstruction of the spiral (right) and the three types of numerical analysis performed on the data (left). (B) Digitized picture of a spiral specimen obtained from a patient with tremor showing the form and dimension of the spiral template. The initial radius (r) was 10.385 mm (i.e. 54 pixels) with an incremental change of 10.385 mm in radius between turns. The 125 mm × 125 mm square that contained the spiral drawing was digitized at a resolution of 650 × 650 pixels.

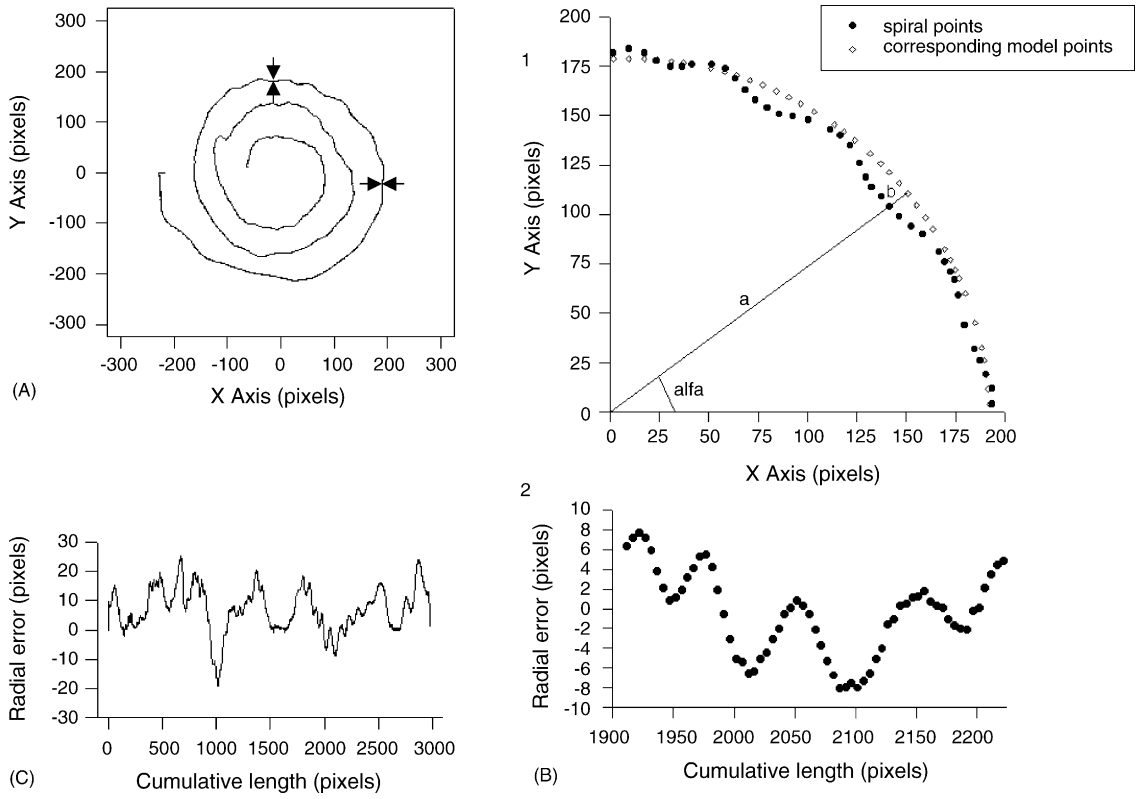

Fig. 2. (A) Spiral reconstituted from the digitized picture showed in Fig. 1B. Note the good similitude with the original image. (B, 1) Enlargement of the spiral sector located between the arrows in part (A). For the sake of clarity, only a 10% of the spiral points represented in (A) are shown. Knowing the spire to which it pertains and the angle that it forms with the x-axis (alfa), it is possible to calculate the corresponding model spiral point (white dots) for each spiral point (black dots). The radial error is signalled with the small letter b. (2) Transformation of the spiral sector shown in part (B, 1). The spatial co-ordinates of each spiral points are substituted for another pair in which the x-value is the spiral length from the origin and the y-value is the radial error. (C) Complete transformation of the spiral represented in part (A).

classified by spires. This was accomplished representing spiral pixels on the computer screen according to the angle that they form with the x-axis (range from 0° to 360°) and the distance from the origin (i.e. polar co-ordinates or radius-angle transformation, Pullman, 1998). This allowed to a human operator to delimit the limits of each spire and then the computer classified the pixels accordingly.

Once the computer determined the spire to which it pertained, it was possible to calculate for each spiral pixel the difference between its distance from the origin and the distance of the corresponding model spiral point (i.e. the point of the model situated at the same spire and angle that a given spiral pixel). This difference was called "radial error" (RE) (Fig. 2B, 1).

Finally, spirals were reconstructed beginning with the pixel pertaining to the first spire and forming the lowest angle with the x-axis. Subsequent pixels were selected in basis to its proximity with the last pixel orderly. At the end, a set of m pairs of x, y co-ordinates values $\{(\mathrm{Xs}, \mathrm{Ys})\} = \{(\mathrm{Xs}_0, \mathrm{Ys}_0), (\mathrm{Xs}_1, \mathrm{Ys}_1), \ldots, (\mathrm{Xs}_{m-1}, \mathrm{Ys}_{m-1})\}$ were obtained.

2.3. Transformation of the spiral

Each pair of x, y co-ordinates representing the successive pixels of the spiral $\{(\mathrm{Xs}, \mathrm{Ys})\}$ were substituted by another pair of x, y co-ordinates (Xt, Yt). For a given n pair of x, y spiral co-ordinates $(\mathrm{Xs}_n, \mathrm{Ys}_n)$, being $0 < n \leq m$, Xt_n was the length of the spiral segment drawn by the subject from $(\mathrm{Xs}_0, \mathrm{Ys}_0)$ to the pixel which was being transformed $(\mathrm{Xs}_n, \mathrm{Ys}_n)$ and Yt_n was the corresponding radial error (Fig. 2). The pair $(\mathrm{Xt}_0, \mathrm{Yt}_0)$ was equal to (0, 0).

In order to apply the fast Fourier transform (FFT), the increment in the Xs′ values of the input signal must always be the same (i.e. the sampling interval must be constant). Since this was not the case in the set of $\{(\mathrm{Xt}, \mathrm{Yt})\}$ data obtained with the above descripted procedure, another set of data $\{(\mathrm{Xt}', \mathrm{Yt}')\}$ was constructed from them. The values of Xt′ were increased one pixel each time; the series began from 0 and extended to the largest integer, less or equal to the last value of Xt. For a given Xt'_n, the Yt'_n value was calculated by linear interpolation of the Yt values of the Xt co-ordinates flanking Xt'_n.

2.4. Mathematical analysis

Analysis of spiral specimens was performed in three different ways. Firstly, the cross correlation coefficient ($K_{\mathrm{s,m}}$) between the subject spiral picture and the model spiral picture (Gonzalez and Woods, 1992) was calculated

$$K_{s,m} = \frac{\sum_{x,y}[(g_{subject}(x, y) - G_{subject})(g_{model}(x, y) - G_{model})]}{\sqrt{\sum_{x,y}(g_{subject}(x, y) - G_{subject})^2 \sum_{x,y}(g_{model}(x, y) - G_{model})^2}} \quad (1)$$

$g_{subject}(x, y)$ is a function that returns a value of 1 when the pixel (x, y) pertains to the spiral drawn by the subject. When the pixel (x, y) pertains to background, the value of the function is 0. Equally, $g_{model}(x, y)$ is 1 when the pixel (x, y) pertain to the print template and 0 when the pixel (x, y) correspond to background.

$G_{subject}$ is the arithmetic mean value of $g_{subject}(x, y)$. G_{model} is the arithmetic mean value of $g_{model}(x, y)$

$$G_{subject} = \frac{\sum_{x,y} g_{subject}(x, y)}{n} \quad (2)$$

$$G_{model} = \frac{\sum_{x,y} g_{model}(x, y)}{n} \quad (3)$$

n is the total number of pixels (i.e.: 650×650).

The normalised cross correlation is a standard method of estimating the degree to which two images are correlated. The coefficient is bounded by -1 and 1. The bounds indicating maximum correlation and 0 indicating no correlation. A high negative value indicates a high correlation but of the inverse of one of the series.

Secondly, the mean (RE_{mean}) and standard deviation ($RE_{S.D.}$) of the radial error was calculated. Finally, the transformed spiral $\{(Xt', Yt')\}$ was spectrally analysed by means of the FFT. The total longitude of the spiral, which is equal to the number of data points (N) of the series $\{(Xt', Yt')\}$, was also computed—see "Transformation of the spiral". Spectral analysis was performed on all the $\{(Xt', Yt')\}$ series—i.e. the complete spiral transformation and, it was also performed, on each one of the six segments of 180° in which the spiral can be divided (Fig. 3). Before applying the FFT to a particular $\{(Xt'_n, Yt'_n)\}$ series, the RE_{mean} was subtracted from each Yt'_n value. Then, Yt'_n values were multiplied by a Hamming window and the spatial series was zero padded until completing 2^{13} samples.

After applying the FFT, the periodogram (P), which represents the spectral power of the spatial series for every frequency bin, was calculated as follows (Timmer et al., 1996)

$$P = \frac{2}{N}(FT_{mag})^2 \quad (4)$$

where N is the number of data points and FT_{mag} is the magnitude of the Fourier transform in polar notation. The expression is multiplied by a factor of 2 in order to include the spectral power of negative frequencies.

The maximum power (W_{max}), the total power (W_{total}), the frequency when the power was to its maximum (F_{max}) and the frequency which divided the power spectrum area in two equal portions (F_{med}) – i.e. median frequency – were determined for both, the periodogram corresponding to the analysis of the spirals as a whole and also for those obtained dividing the spirals by sectors. Spectrum area was calculated by numerical integration of the periodogram using the trapezoidal rule.

2.5. Simulation of tremulous spirals

The methodology of spiral analysis we have developed relies fundamentally on the FFT analysis of a numerical series where the independent variable is not the time. Moreover, the x-variable is not really independent but it is a calculated variable (i.e. the accumulative distance covered during the spiral drawing) that depends on the drawing velocity of the subject and on the existence of one or more periodic oscillations superimposed on the main movement of the upper arm following the path defined by the spiral template. This makes the interpretation of the spectral analysis less intuitive than when FFT is applied to a temporal series. In order to found theoretically our spiral analysis and to

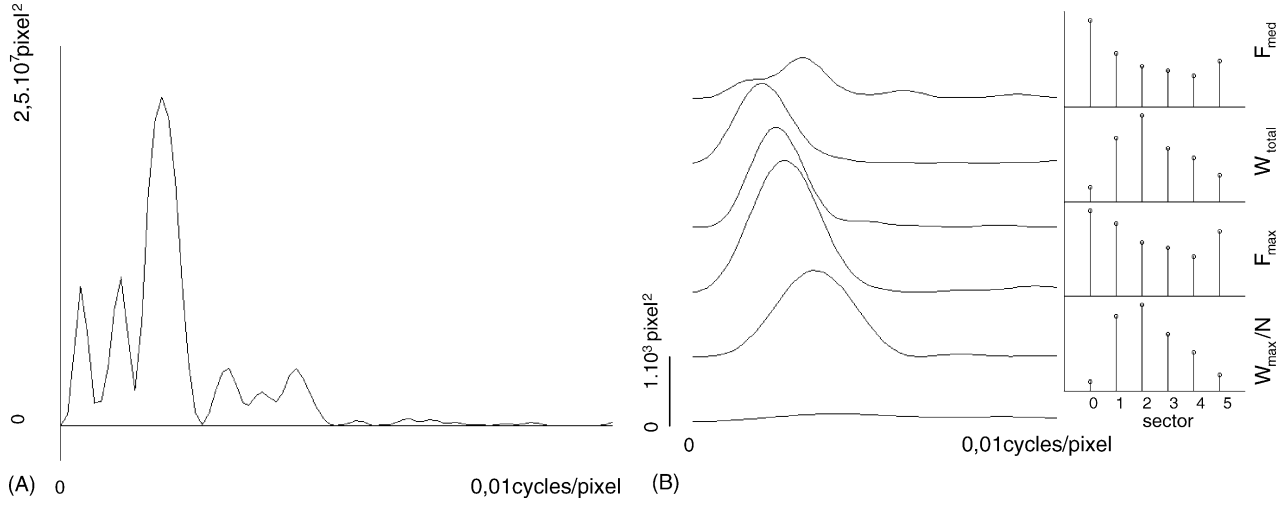

Fig. 3. (A) Fourier analysis of the spiral represented in Figs. 1 and 2. Note the presence of multiple spectral peaks although one of them is clearly dominant. (B) Fourier analysis by sectors of the spiral represented in Figs. 1 and 2. In contrast with the spectrum of the whole spiral in part (A), the sectorial analysis make clear the existence of a unique spectral peak, whose frequency decreases non-linearly along the sectors. Bar graphics are normalised respects to the maximum value of W_{max}/N, F_{max}, W_{total} and F_{med}, respectively.

test its numerical results, we have designed a computer program that simulates the drawing of a spiral by a subject with tremor. The simulation allows changing the drawing velocity and the number and characteristics of periodic oscillations added to the drawing spiral movement. The mathematical details of the simulation are given in Appendix A.

2.6. Computer programming and numerical integration of simulated tremulous spirals

Spiral specimens were digitized with the aid of an HP ScanJet 4100C (Hewelett Packard Company) scanner, operating the Windows 98 (Microsoft, Redmond, Washington) HP Precision Scan LT software (Hewelett Packard Company, 1998). 24-bits bitmap files were decodified and displayed in a 8-bits graphic screen using the public domain QuickBasic program BMP24BITS.BAS v1.0 written by Yousuf Philips (YPI BASIC Programming Inc., 1999) downloaded from the web site http://members.xoom.com/Philipz (last access 13 February 2001). Spiral image processing, data analysis and simulation of tremor spirals were performed in a Pentium II-based personal computer, which was also programmed using the QuickBasic environment (Microsoft). In the construction of theoretical spirals, dt was 0.01 s and da was 0.0001 rad.

2.7. Subjects and clinical rating scale

Twenty-four healthy subjects and 31 subjects with action tremor (one patient with hyperthyroidism, one patient with a likely benign small tumour in the third ventricle and the remaining patients with essential tremor) participated in this study after giving their informed consent. The study was approved by the ethical committee of the Government of the autonomous region of the Balearic Islands. There were 12 males and 12 females with an average age of 53.2 years (range 35–79 years) in the control group. Healthy subjects were recruited among partners of patients with tremor and medical staff. Patient's group was constituted by 17 males and 14 females. Their average age was of 65.5 years old (range 24–81). Patients on treatment did not stop their medication before joining the study. Spirography specimens were rated independently by three neurologists who were blinded to the subject's category (control or patients). Each ratter ascribed each spiral a score from 0 (normal) to a possible maximum of 10 (extremely tremulous) (Bain et al., 1993).

2.8. Statistical analysis

Statistical analysis was performed with the personal computer program SPSS 8.0.0 for Windows (SPSS Inc., 1997). Normal subjects were separated into two groups according to their age: the first group included subjects younger than 50 years and the second group all older subjects. This division of the control group allowed studying the change in the drawing performance with the age in healthy people. Data from patients were compared with data from controls older than 50 years with the aim to eliminate differences in the mean age between both groups. Comparison of the mean of the experimental variables $K_{s,m}$, RE_{mean}, $RE_{S.D.}$, W_{max} and W_{total} was performed using the Mann–Whitney U-test. The change in the spectral variables (W_{max}, W_{total}, F_{max} and F_{med}) depending on the sector of the spiral drawing was studied by a two-way between by within subject's analysis of variance (ANOVA) design. The between subjects factor was the Group factor (two levels: controls $\leq$50 years old versus controls >50 years old; controls >50 years old versus patients). The within subject factor was the spiral sector (six levels). Spearman's rho correlation coefficient was used to study the correlation between the clinical spiral score and the variables derived from the computational analysis. Probability values of statistical test found are stated in the text; a $p < 0.05$ was considered statistically significant. ROC curves were calculated in order to compare the usefulness of the different parameters obtained from the analysis of the spiral drawing in the diagnosis of action tremor. ROC curves were elaborated with custom made software written in QuickBasic.

3. Results

3.1. Theoretical spirals

3.1.1. Drawing velocity

Fig. 4 shows the effect of the drawing velocity on the spectral characteristics of the spirals. As the velocity was increased from 150 to 350 pixels/s, fewer oscillations were drawn per longitude unit and the corresponding spectral peak was displaced to the left accordingly. The total spiral longitude and, therefore, the number of data points (N) also decreased with the increase of the drawing velocity but, as expected, the total power (W_{total}) did not change since the periodogram was normalised by N. However, in spite of the normalisation of the periodogram stated in Eq. (4), there was a progressive reduction in the amplitude of the spectral peak (W_{max}). Division by N made that W_{max} of spiral spectra did not change when the drawing velocity was modified.

3.1.2. Tremor amplitude

The augment of tremor amplitude was reflected in a roughly linear increase in the value of W_{total} (Fig. 5C, 3). In contrast, W_{max} grew in parallel with the exponential increase in N. Again, dividing W_{max} by N brings the curve near to a straight line (Fig. 5C, 2).

3.1.3. Presence of a second oscillation

The presence of a second periodic oscillation caused a profound change in the form of the spiral and in its spectrum. The increase in the amplitude of the fast oscillation made that the spectral peak corresponding to the fundamental one displaced to lesser spatial frequencies although neither the drawing velocity nor the frequency of oscillations was changed (Fig. 6C, 4). This effect was due to the augment in the spiral longitude that supposed the presence of a second oscillation; in this case, the same number of cycles of the main oscillation was drawn in a greater spiral longitude (Fig. 6). As expected, both W_{total} and the quotient W_{max}/N was about the same irrespective of the amplitude of the fast oscillation (Fig. 6C, 2 and 3).

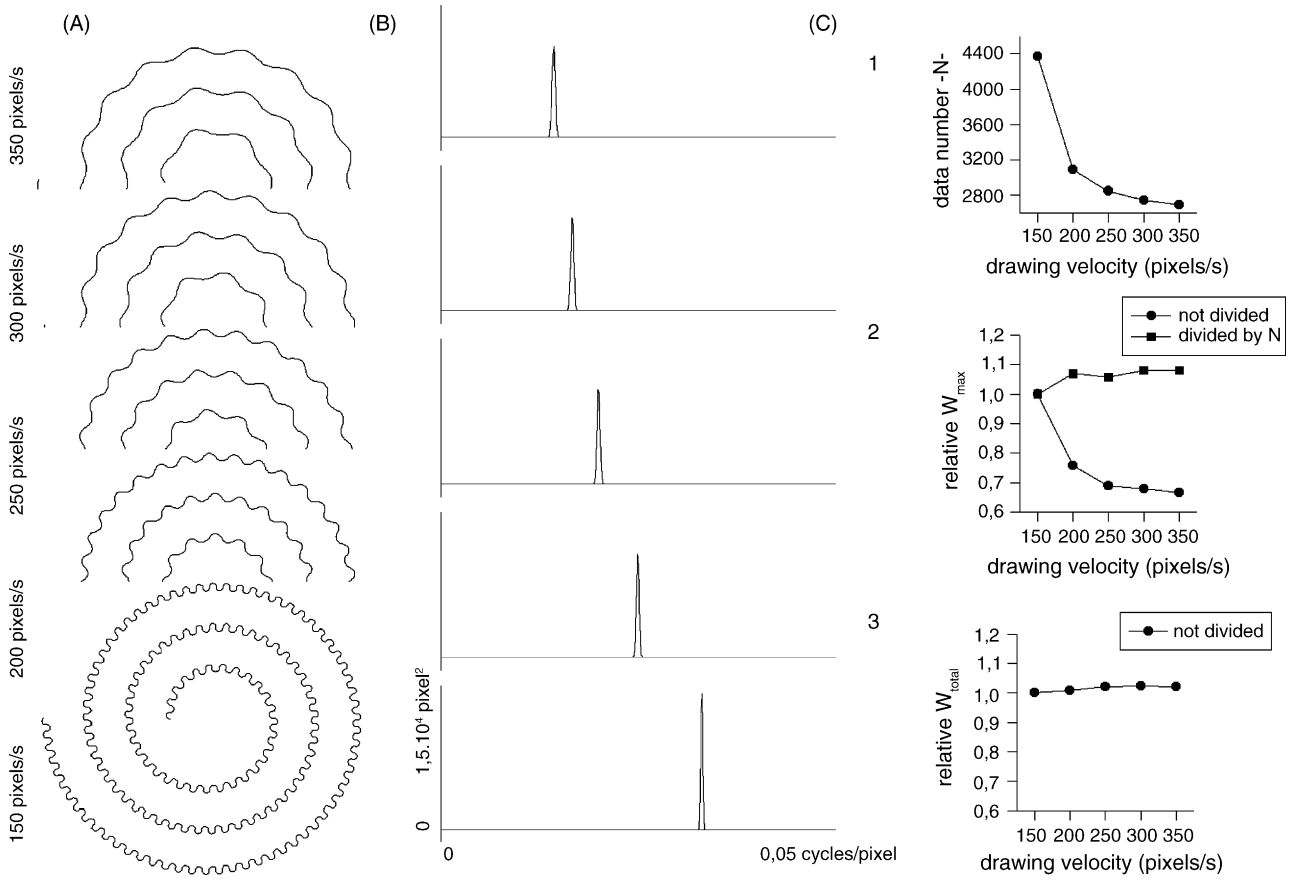

Fig. 4. Effect of the drawing velocity on the characteristics of the spectral analysis of spirals. (A) Change in the form of spirals as the drawing velocity was increased from bottom to top. In all spirals, the superimposed oscillation has a frequency of 5 Hz and amplitude of 5 pixels. (B) Corresponding spectra of the spirals represented in part (A). (C) From bottom to top, change in W_{total}, W_{max} and in data number (the value of which is equal to the spiral length) with drawing velocity. Note that division of W_{total} by N (i.e. data number) and of W_{max} by N^2 (instead of N, as usual, see Section 2) made that the value of these variables did not depend on the drawing velocity.

3.1.4. Tremor direction

The consequence of changing the orientation of the periodic oscillation is illustrated in Fig. 7. When the oscillation followed the radius of the spiral, only one peak was present in the periodogram (Fig. 7A, 1–3). On the contrary, there were two small spectral peaks when the orientation of the oscillation was perpendicular to the x-axis (Fig. 7B, 1–3). Nevertheless, the analysis of the spiral by sectors instead of as a whole revealed the existence of only one peak in the periodograms corresponding to each one of the six sectors (Fig. 7A, 4 and Fig. 7B, 4). Moreover, the spectral parameters – W_{max}/N, W_{total}, F_{max}, F_{med} – did not change between the different sectors and their values were similar to that obtained when the oscillation followed the spiral radius.

3.1.5. Variable drawing velocity and variable tremor direction

It is well known that the drawing velocity is not constant but varies strongly with the instantaneous curvature according to the so-called "two-thirds" power law (see Appendix A). When this phenomenon was taken into account in the spiral simulations, there was a dramatic change in the corresponding periodogram (Fig. 8), especially if the oscillation was perpendicular to the x-axis (Fig. 8C, 1–3). In that case, the single peak presented when the drawing velocity was constant and the oscillation was parallel to the spiral radius (Fig. 8A, 1–3) was substituted by a spectrum with multiple and small peaks. However, the FFT analysis of the spiral by sectors revealed one peak in the corresponding periodograms, although its frequency (F_{max} and F_{med}) decreased in parallel with the increase in the drawing velocity (Fig. 8C, 4 and 5). As expected, W_{max}/N and W_{total} did not change between the different sectors since the oscillation amplitude was the same in all simulated conditions (Fig. 8A–C, 5); their values were similar to that obtained in the constant velocity condition (Fig. 7A, 4 and 5).

3.2. Control spirals

All subjects were able to complete the spiral; thus, all the steps of the present method of analysis (i.e. cross-correlation analysis, radial error analysis and FFT of the reconstructed spiral) could be performed in all spiral specimens. The value of the variables obtained from the analysis of the spirals as a whole is summarised in Table 1. There were statistical significant differences between age-groups (controls $\leq$50 years old versus controls >50 years old) in RE_{mean} ($p = 0.026$) and W_{max}/N ($p = 0.018$). The

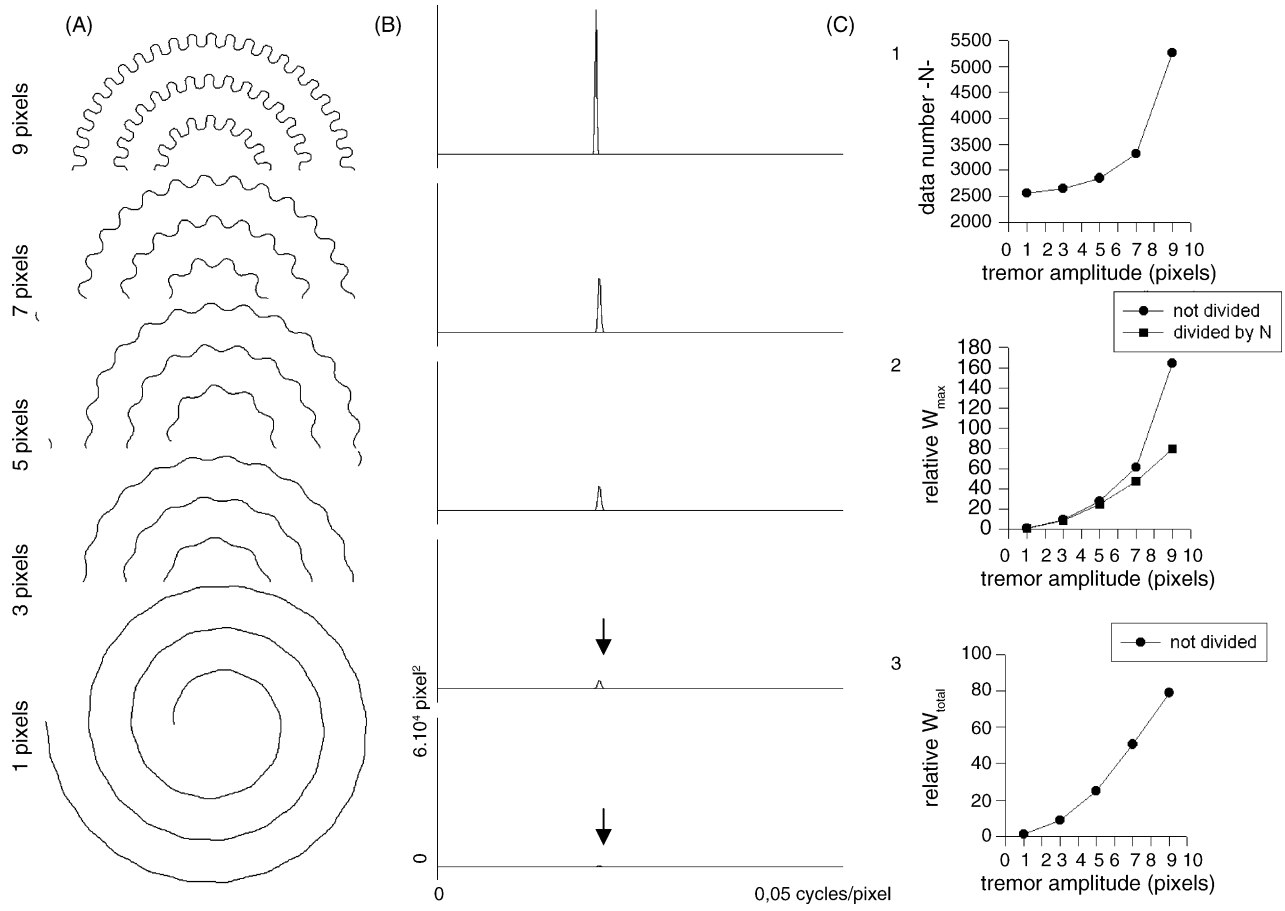

Fig. 5. Effect of the tremor amplitude on the characteristics of the spectral analysis of spirals. (A) Change in the form of spirals as the tremor amplitude was increased from bottom to top. In all spirals, the superimposed oscillation has a frequency of 5 Hz and the drawing velocity was 250 pixels/s. (B) Corresponding spectra of the spirals represented in part (A). Arrows point out the barely visible spectral peak in the last two graphics. (C) From bottom to top, changes in W_{total}, W_{max} and in data number (the value of which is equal to the spiral length) with tremor amplitude. Note that division of W_{total} by N (i.e. data number) and of W_{max} by N^2 made that the value of these variables increased almost linearly with the tremor amplitude.

significance of W_{total} was just at the statistical threshold without reaching it ($p = 0.050$).

Five subjects pertaining to the group with an age older than 50 presented a well-defined peak in the periodogram whereas only one of the youngest control subjects presented a single spectral peak. Consistent with the low incidence of well-defined peaks in the individual spectra, the grand-average of periodograms pertaining to controls >50 years old showed a spectral peak although with a broad morphology. There was not any recognisable peak in the grand-average of periodograms from controls ≤50 years old (Fig. 9A).

Table 1
Values of experimental variables

	Controls ≤50 years old	Controls >50 years old	Patients
Age	41.1 ± 4.1	65.4 ± 7.2	65.5 ± 13.5
n	12	12	31
Data number (N)	3288 ± 372	3540 ± 425	4214 ± 1219
$K_{s.m}$	0.35 ± 0.07	0.30 ± 0.07	0.19 ± 0.11
RE_{mean}	2.25 ± 0.59	2.82 ± 0.77	5.45 ± 3.06
$RE_{S.D.}$	1.53 ± 0.42	1.92 ± 0.68	4.01 ± 2.39
W_{max}/N	0.42 ± 0.32	1.07 ± 1.06	3.32 ± 4.02
W_{total}	2.31 ± 1.29	4.15 ± 2.99	17.54 ± 18.34
F_{max} (10^{-3})	1.40 ± 0.73	0.78 ± 0.42	0.85 ± 0.55
F_{med} (10^{-3})	2.66 ± 1.31	1.95 ± 0.93	2.65 ± 1.47
$^{sec}W_{max}$/N	1.02 ± 0.49	2.16 ± 2.01	9.74 ± 15.97
$^{sec}W_{total}$	1.76 ± 0.61	3.21 ± 2.00	16.36 ± 21.35
Clinical score	0.80 ± 0.43	1.36 ± 0.90	4.75 ± 2.69

3.2.1. Spectral analysis of spirals by sectors

In contrast with the results obtained from the spectral analysis of the spiral as a whole, the FFT analysis of the spiral by sectors revealed the presence of a dominant peak in the periodogram of at least one spiral sector in virtually all controls. The presence of a periodic oscillation in the healthy subjects with independence of their age was more evident when the periodograms were averaged by sectors. Then, a spectral peak was visible in all sectors in both age-groups (Fig. 10A). The ANOVA showed a statistically significant non-linear decrease of F_{max} and F_{med} within sectors ($p < 0.001$ in both parameters) (Fig. 10A). There was also found that F_{max} and F_{med} were significantly smaller in the group of normal subjects older than 50 than in the youngest controls ($p = 0.018$ and $p = 0.021$, respectively). W_{max}/N and W_{total} did not change within sectors but there was a statistically significant

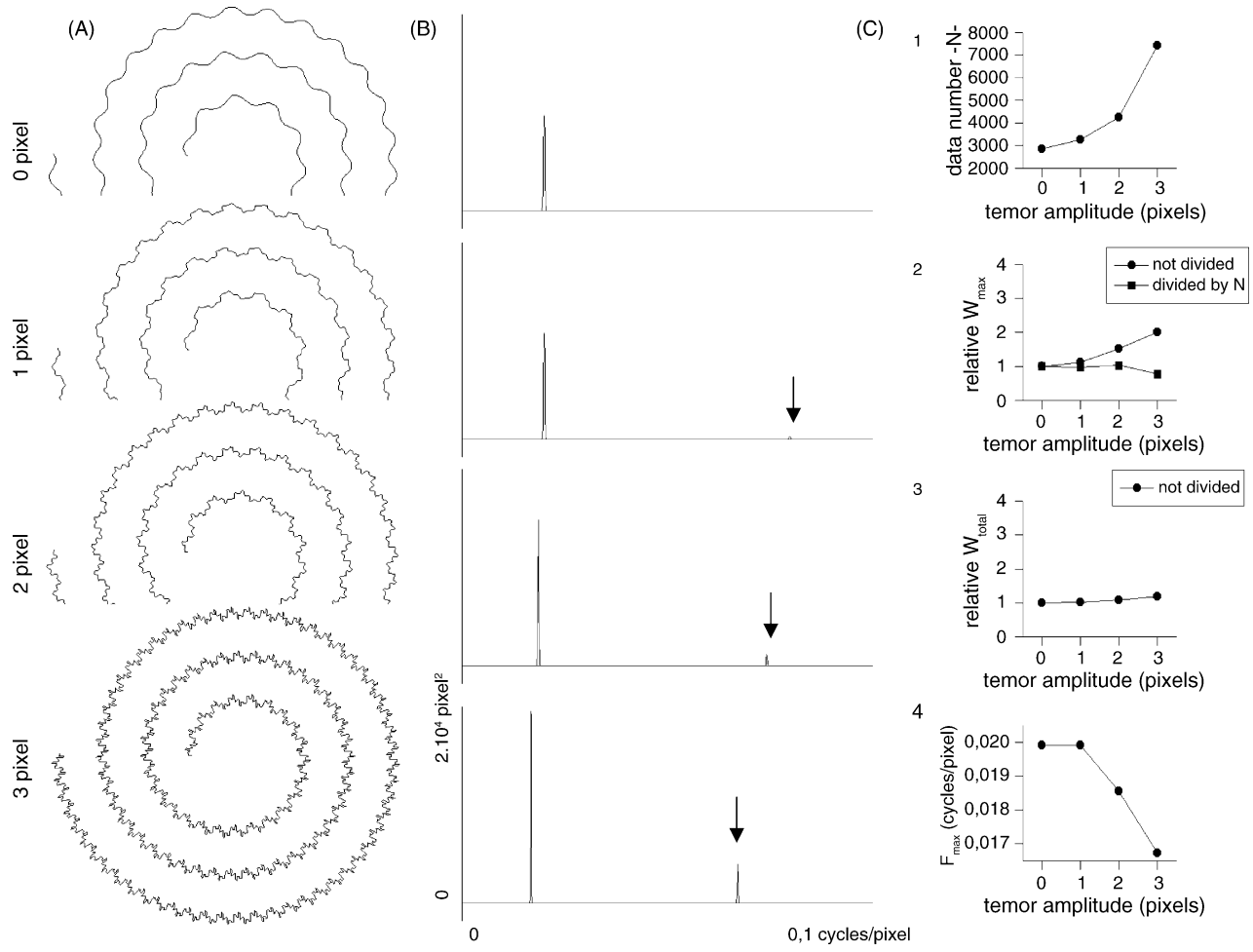

Fig. 6. Effect of the presence of a second periodic oscillation on the characteristics of the spectral analysis of spirals. (A) Change in the form of spirals as the amplitude of the fast oscillation was increased from top to bottom. In all spirals, the main oscillation has a frequency of 5 Hz and amplitude of 5 pixels. The second oscillation has a frequency of 20 Hz and its amplitude increased from 0 pixels (top) to 3 pixels (bottom). The drawing velocity was 250 pixels/s in all spirals. (B) Corresponding spectra of the spirals represented in part (A). Arrows point out the spectral peak corresponding to the fastest oscillation; it was barely visible when the amplitude was less than 3 pixels. (C) From bottom to top, changes in F_{max}, W_{total}, W_{max} and in data number (its value is equal to the spiral length) with the amplitude of the fast oscillation. Notice that F_{max} (i.e. the frequency of the main oscillation) decreased as the amplitude of the second oscillation increased and that division of W_{total} by N (i.e. data number) and of W_{max} by N^2 made that the value of these variables remained almost invariable.

increase in the value of these variables in the control group constituted by people older than 50 respect to the youngest controls ($p = 0.001$ and $p < 0.001$, respectively). No significant interaction was observed from F_{max}, F_{med}, W_{max}/N and W_{total} between the two experimental factors. Since the ANOVA did not detect differences in W_{max}/N and W_{total} among sectors, the mean of the six values of these variables was calculated for each normal subject ($^{sec}W_{max}/N$ and $^{sec}W_{total}$, respectively). The Mann–Whitney U-test confirmed that $^{sec}W_{max}/N$ and $^{sec}W_{total}$ were significantly greater in control subjects older than 50 ($p = 0.015$ and $p = 0.006$, respectively) (Table 1).

3.3. Tremor spirals

Twenty-eight of the 31 patients studied were able to complete the test in such a way that it was possible to fully reconstitute the spiral and to perform the complete analysis of the drawing. It was possible to calculate the radial error and the cross-correlation coefficient in one of the remains three patients whereas in the others two, only the cross-correlation coefficient could be determined since the spiral drawing was very fragmented. There were statistically significant differences in W_{max}/N ($p = 0.007$), W_{total} ($p < 0.001$), $K_{s,m}$ ($p = 0.003$), RE_{mean} ($p = 0.001$) and $RE_{S.D.}$ ($p < 0.001$) between patients and controls older than 50 (Table 1). In contrast to that observed in the oldest controls, there was not a clear spectral peak in the averaged periodogram of tremor spirals (Fig. 9B). However, when considered individually, 14 out of 28 patient's spiral spectra showed a dominant peak in its periodogram (Fig. 3A). The remaining spectra showed no peaks or several of them with similar amplitude.

3.3.1. Spectral analysis of spirals by sectors

In a similar way to that observed in control subjects, the FFT-analysis of the spiral by sectors revealed a single peak in at least one of the corresponding periodograms in all patients. Moreover, the spectrum obtained after averaging all the periodograms corresponding to the same sector showed a single peak, the frequency of which decreased non-linearly along the

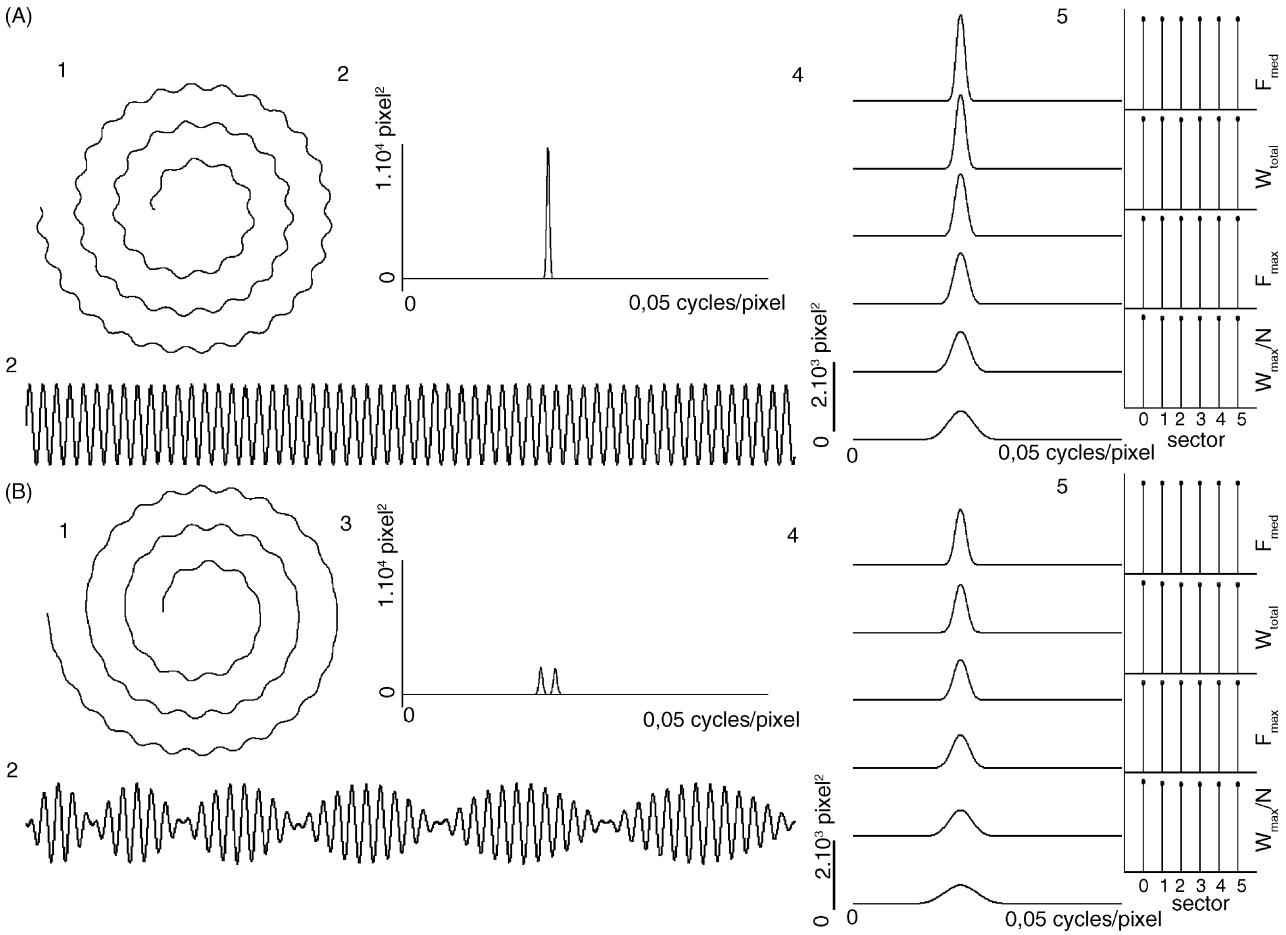

Fig. 7. Effect of the spatial orientation of the tremor on the spectral characteristics of the spirals. (A) Tremor parallel to the spiral radius: (1) form of the simulated tremulous spiral; (2) graphic representation of the transformation of the spiral; (3) spectrum of the whole spiral; (4) spectra of the six sectors of the spiral; and (5) bar graphics representing the value of the spectral variables by sectors. Bar graphics are normalised respect to the maximum value of W_{max}/N (bottom), F_{max}, W_{total} and F_{med} (top). (B) Tremor perpendicular to the *x*-axis: (1) form of the simulated tremulous spiral; (2) graphic representation of the transformation of the spiral; (3) spectrum of the whole spiral; (4) spectra of the six sectors of the spiral; and (5) bar graphics representing the value of the spectral variables by sectors. Bar graphics are normalised respect to the maximum value of W_{max}/N (bottom), F_{max}, W_{total} and F_{med} (top), respectively. In parts (A and B) the tremor has a frequency of 5 Hz and an amplitude of 5 pixels; the drawing velocity was 250 pixels/s.

sectors just like to that observed in normal subjects (Fig. 9). The ANOVA showed statistically significant differences in F_{max} and F_{med} ($p < 0.001$ and $p = 0.002$, respectively) within sectors but not between patients and controls. W_{max}/N and W_{total} did not change within sectors but there was a statistically significant increase in the value of these variables in the patients group respect to control subjects older than 50 ($p = 0.007$ and $p < 0.001$, respectively). No significant interaction was observed from F_{max}, F_{med}, W_{max}/N and W_{total} between the two experimental factors. Since the ANOVA did not detect differences in W_{max}/N and W_{total} among sectors, the mean of the six values of these variables was calculated for each patient ($^{sec}W_{max}/N$ and $^{sec}W_{total}$, respectively). The Mann–Whitney *U*-test confirmed that $^{sec}W_{max}/N$ and $^{sec}W_{total}$ were significantly greater in the patients group than in the controls older than 50 ($p = 0.002$ and $p < 0.001$, respectively) (Table 1).

Table 2
Spearman's rho cross correlation coefficients and ROC curve area

	Spearman's rho cross correlation coefficients			ROC curve area
	Controls and patients	Controls	Patients	Controls and patients
$K_{s,m}$	−0.593 ($p < 0.001$)	−0.337 ($p = 0.107$)	−0.552 ($p = 0.002$)	0.173
RE_{mean}	0.735 ($p < 0.001$)	0.375 ($p = 0.071$)	0.608 ($p = 0.001$)	0.860
$RE_{S.D.}$	0.791 ($p < 0.001$)	0.178 ($p = 0.406$)	0.799 ($p < 0.001$)	0.889
W_{max}/N	0.657 ($p < 0.001$)	0.379 ($p = 0.068$)	0.432 ($p = 0.021$)	0.836
W_{total}	0.797 ($p < 0.001$)	0.356 ($p = 0.088$)	0.761 ($p < 0.001$)	0.879
$^{sec}W_{max}/N$	0.644 ($p < 0.001$)	0.008 ($p = 0.972$)	0.581 ($p = 0.001$)	0.841
$^{sec}W_{total}$	0.795 ($p < 0.001$)	0.100 ($p = 0.640$)	0.816 ($p < 0.001$)	0.912
Clinical score	–	–	–	0.889

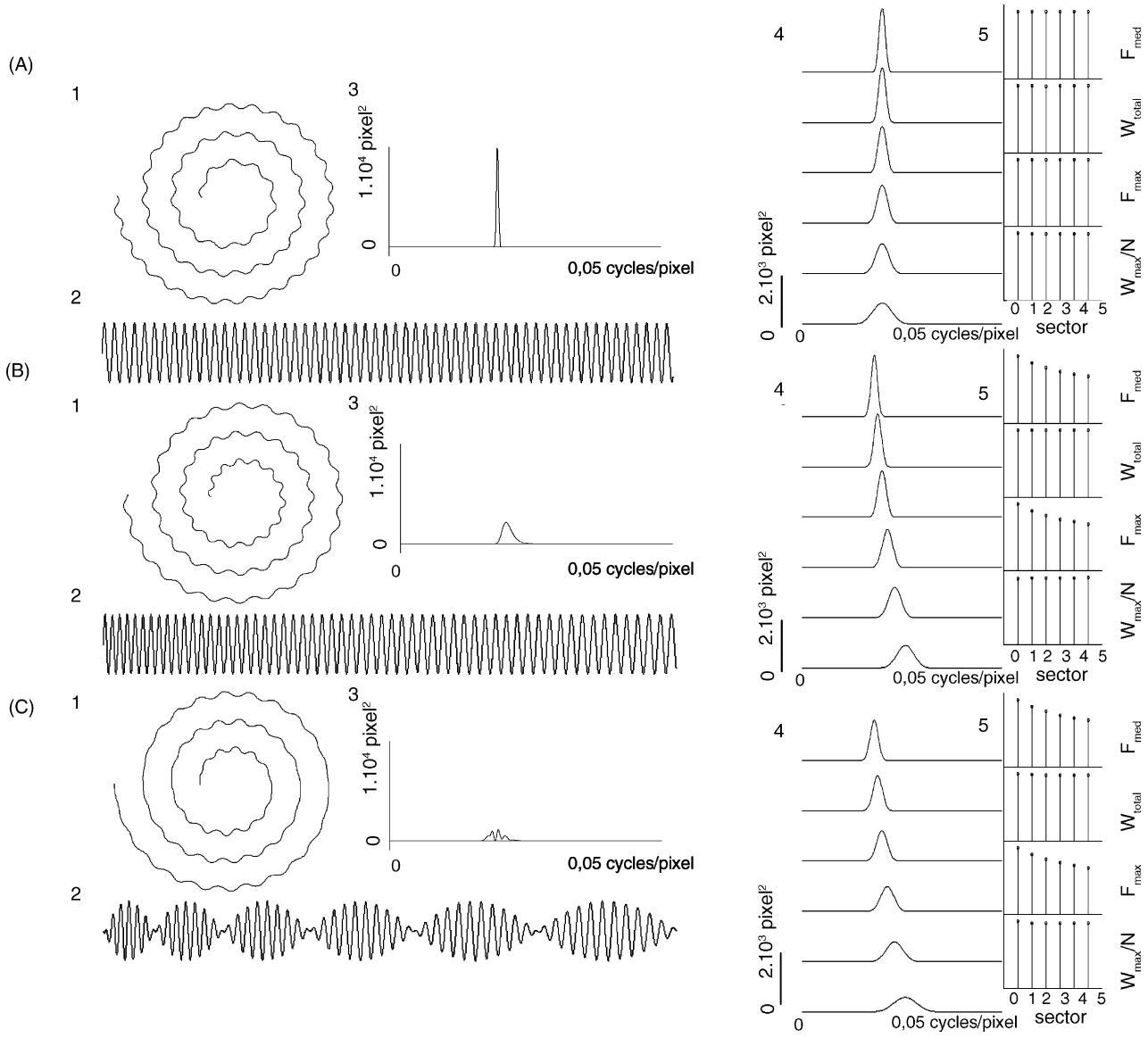

Fig. 8. Effect of a variable drawing velocity on the spectral characteristics of the spirals. (A) Constant drawing velocity of 250 pixels/s and tremor parallel to the spiral radius: (1) form of the simulated tremulous spiral; (2) graphic representation of the transformation of the spiral; (3) spectrum of the whole spiral; (4) spectra of the six sectors of the spiral; and (5) bar graphics representing the value of the spectral variables by sectors. Bar graphics are normalised respect to the maximum value of W_{max}/N (bottom), F_{max}, W_{total} and F_{med} (top), respectively. (B) Variable drawing velocity according to the "two-thirds power law" and tremor parallel to the radius of the spiral: (1) form of the simulated tremulous spiral; (2) graphic representation of the transformation of the spiral; (3) spectrum of the whole spiral; (4) spectra of the six sectors of the spiral; and (5) bar graphics representing the value of the spectral variables by sectors. Bar graphics are normalised respect to the maximum value of W_{max}/N (bottom), F_{max}, W_{total} and F_{med} (top), respectively. (C) Variable drawing velocity according to the "two-thirds power law" and tremor perpendicular to the radius of the spiral: (1) form of the simulated tremulous spiral; (2) graphic representation of the transformation of the spiral; (3) spectrum of the whole spiral; (4) spectra of the six sectors of the spiral; and (5) bar graphics representing the value of the spectral variables by sectors. Bar graphics are normalised respect to the maximum value of W_{max}/N (bottom), F_{max}, W_{total} and F_{med} (top), respectively. In parts (A–C) the tremor has a frequency of 5 Hz and an amplitude of 5 pixels; the mean drawing velocity was 250 pixels/s which was obtained setting the "gain factor (g)" – Appendix A – to 48.

3.4. Correlation with clinical rating score

The Spearman's rho correlation coefficients obtained among the different mathematical variables studied and the mean score given by the ratters are shown in the Table 2. In general, there was a good correlation between the computational analysis and the clinical judgement of spiral specimens (rho coefficients greater than 0.7) except in the case of $K_{s,m}$. These high values of correlation coefficients were mainly due to the spirals drawn by the patients because when the statistical analysis was carried out considering control subjects and patients separately, there was not found any significant correlation in the control group (Table 2).

3.5. ROC analysis of computational variables

The results of the numeric integration of the ROC curves corresponding to spiral parameters obtained from the computational analysis and from the clinical evaluation of drawings (mean score of the three ratters) are shown in Table 2. With the

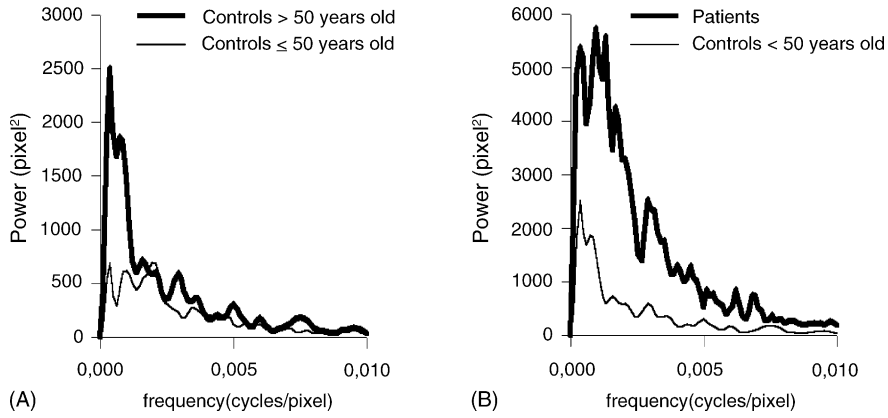

Fig. 9. Grand average of periodograms corresponding to the analysis of the complete spirals. (A) Averaged periodogram of control subjects younger than 50 (thin line) vs. control subjects older than 50 (thick line). (B) Averaged periodogram of patients (thick line) vs. control subjects older than 50 (thin line).

exception of $K_{s,m}$, all the other variables had an area-under-the-curve similar to that found for the clinical rating scale.

4. Discussion

We have developed a new method of quantification of the drawing of an Archimedes spiral. The method has two clearly distinguishable parts. One is the processing of the spiral picture from its bitmap file to an arranged set of pixels that reconstructs the temporal sequence following which the spiral was drawn by the subject in an ordinal scale. The visual comparison between the reconstructed spirals and they original pictures, and the consistent results obtained both in patients and controls, point out that the present computer procedure achieved the goal of reconstructing the subjects spiral acceptably.

The spiral specimens, which measured 125 mm × 125 mm, were transformed in a 650 × 650 pixels bitmap file. Thus, the scanning procedure could individualise two points 0.1923 mm apart (i.e. 125 mm/650 pixels). This implied that the digitization rate was high enough to reproduce faithfully a tremulous oscillation with a spatial frequency up to about 1 cycle/mm (considering the unrealistic case that the lines drawn by the subjects were of one pixel width and, accordingly, one cycle extended along 5 pixels). This extremely high digitizing rate guaranteed that the method was not contaminated by any aliasing phenomena, moreover, if we take into account that there was not virtually any spectral power at frequencies greater than 0.05 cycles/pixel.

Three different types of mathematical analysis of the spiral data were designed with the aim to cover all the possible drawing performances. Firstly, the spatial cross-correlation coefficient between the subject's spirals and the spiral template was calculated. The calculus of this coefficient only required that spiral pixels were segregated from the rest of the bitmap file without any further data manipulation. Despite there were both a statistically significant difference in this parameter between patients and controls older than 50 and a weak, but significant, correlation with the clinical scale score (rho = −0.593, $p < 0.001$), this coefficient was the worst parameter in differentiating patients from control subjects as judged by its performance in the ROC curve analysis. Nevertheless, the spatial cross-correlation coefficient allows to quantify any spiral drawing, even if it is incomplete or too complex to be classified by spires.

Secondly, the distance respect to the corresponding model spiral pixel was determined for each pixel belonging to the spirals drawn by the subjects. The obtaining of this parameter, which was termed "radial error", required the completion of the spiral drawing and that the spiral pixels could be classified by spires. RE_{mean} and $RE_{S.D.}$ were significantly greater in patients than controls. In addition, both variables were highly correlated with the clinical rating score (rho > 0.7, $p < 0.001$) and the value of the area of its ROC curves was virtually identical to that found for the clinical rating procedure. Thus, the determination of the radial error seems to be a good candidate in the searching of an objective method to evaluate the drawing of a spiral since it is highly correlated with the clinical judgement and classified correctly most of the spiral specimens. Nevertheless, radial error does not detect neither the existence of periodic components in the drawing nor changes in the drawing velocity.

Finally, spirals were analysed using the FFT. Spectral analysis was performed after the transformation of spirals in a time-related series in which the independent variable was the cumulative length of the spiral. This election was conditioned to that the cumulative length of the spiral is the sole variable that changes monotonically (i.e. it is always increasing) in a spiral drawing. However, the fact that the "independent" variable is not really independent but depends, among other factors, on the drawing velocity, implies that changes in the spectral variables do not necessarily indicate a change in the characteristics of tremor. With the aim to determine what information about the nature of tremor may be inferred from the spectral analysis of the spiral picture, we have developed a simple mathematical model of the drawing of a tremulous spiral. The model illustrates the complex relationships between the characteristics of tremor and its corresponding FFT analysis. Thus, changes in the drawing velocity, the direction of tremor on respect to the spiral radius and the presence of additional oscillations superimposed on the tremor had profound consequences in the spiral spectrum although the frequency and amplitude of the tremor were invariable along the simulations. We empirically found that these effects could be minimised analysing the spiral by

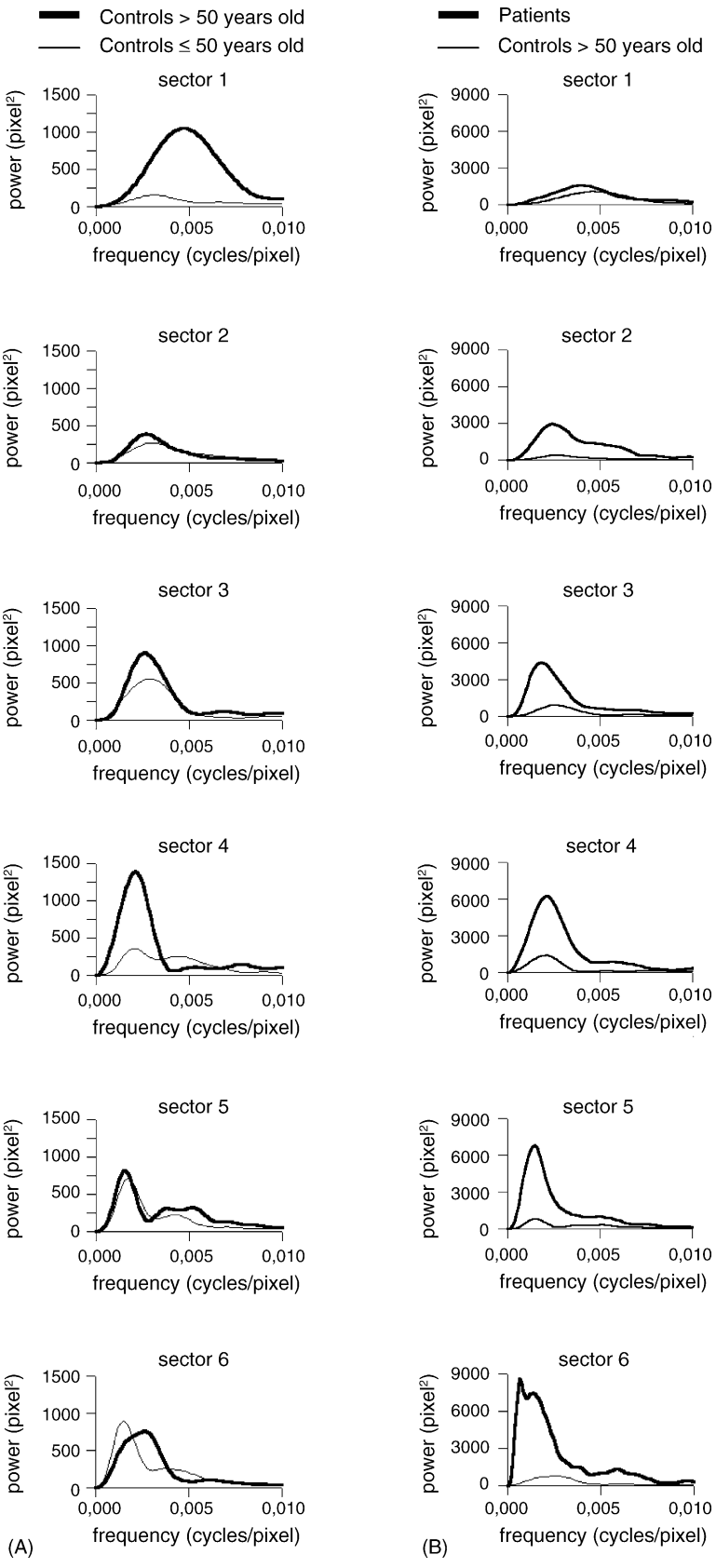

Fig. 10. Grand average of periodograms corresponding to the analysis of the spirals by sectors. (A) Averaged periodogram of control subjects younger than 50 (thin line) vs. control subjects older than 50 (thick line). (B) Averaged periodogram of patients (thick line) vs. control subjects older than 50 (thin line).

sectors, instead as a whole and dividing the value of the peak power (W_{max}) by N (number of data points). In this respect, in the most realistic case simulated (i.e. a variable drawing velocity according to the "two-third power" and presence of a tremulous oscillation perpendicular to the x-axis), the FFT analysis by sectors revealed the presence of a single spectral peak correctly. Its frequency, as expected given the variable drawing velocity, decreased across the sectors. The W_{max}/N of the peak and the W_{total} of the spectra were the same in the six spiral sectors, which was consistent with the fact that the tremor amplitude did not change throughout the simulation.

The Fourier analysis of the control spirals showed the presence of a spectral peak in, as a minimum, one sector periodogram in all the healthy population studied. This finding, which indicate the existence of an oscillating radial deviation in the spiral line traced by healthy subjects, was confirmed by the presence of a spectral peak in the grand average of sectorial periodograms obtained from the control population. The frequency of this peak decrease non-linearly across the sectors. This rhythmic spatial error appears to be more marked in the healthy population older than 50, as judged by the fact that W_{max}/N, W_{total}, ${}^{sec}W_{max}/N$ and ${}^{sec}W_{total}$ were significantly greater in this age-group than in the youngest normal people. The origin of this periodic deviation in the spiral drawing cannot be inferred with certainty from a spiral picture that no contains explicit information about time although it might be expression of the physiologic tremor. This hypothesis is supported by the good agreement between the averaged sectorial periodograms from the control group and the results of our computer simulation of the drawing of a tremulous spiral according the "two-third power law" in the non-linear dependence of the peak frequency respect to the spiral sector. Nevertheless, only the use of a graphic tablet, which give information about time, will allow to find the correct explanation.

The whole spiral spectra of tremor patients revealed the presence of a single peak in only about 50% of the drawings but the FFT-analysis of the tremor spirals by sectors revealed the existence of a single spectral peak in, at least, one of them. The averaged sectorial periodograms, in a similar way to healthy population, showed a peak, the frequency of which decreased non-linearly across the sectors. The magnitude of the decrease could be well fitted by a quadratic polynomial curve with similar parameter values to that found both for spiral computer simulations and for control subjects (data not shown). This fact seems to reveal that in the patients with essential tremor, there is the same exponential relationship between drawing velocity and instantaneous curvature as in healthy people (Lacquaniti et al., 1983) or in Parkinson disease (Longstaff et al., 2003).

W_{max}/N, W_{total}, ${}^{sec}W_{max}/N$ and ${}^{sec}W_{total}$ were significantly greater in the patients group than in the control subjects older than 50. There was also a good cross-correlation between the clinical rating score and both W_{total} and ${}^{sec}W_{total}$ (rho > 0.790 and $p < 0.001$ in both cases). Finally, the ROC curve area of those variables was equal or superior to that found by the clinical rating procedure. Therefore, W_{total} and, specially, ${}^{sec}W_{total}$ seem to be the best spectral parameters in order to quantify the severity of a drawing tremor because of their high correlation with the clinical judgement of spiral performance and their ability to discriminate most of the tremor spirals from control specimens correctly. At this point, it is important to stress that our goal was to develop a quantitative method of analysis of a spiral drawing not a diagnostic test aimed to detect the presence of a pathologic drawing tremor. Thus, the spectral variables that we taken in consideration were the total power and the maximum power of the signal obtained form the spiral specimens irrespective of whether its spectrum contained a peak or not. From the value of these variables, it is not possible to distinguish whether an impairment in spiral drawing is due to tremor or to an arrhythmic error in movement.

Bain et al. (1993) found that the assessment of spirography using a 0–10 clinical tremor severity score was highly correlated with disability as well as with right upper limb postural tremor grades in patients with essential tremor and dystonic tremor. They conclude that spirography provides a "valid and convenient measure of the disability caused by postural tremor". Nevertheless, subjective assessment of spirography has several drawbacks. Firstly, this clinical method has a low interratter reability. Thus, in the study of Bain et al. (1993), the agreement among the different ratters was sometimes only moderate. This finding was further confirmed in a recent study from the same group carried out in patients with tremor due to multiple sclerosis (Alusi et al., 2000). Secondly, it has a low "ceiling effect". This phenomenon is due to that some patients with incapacitating tremors are unable to draw spirals although their tremors could be rated from simple postures and movements (Alusi et al., 2000). These inconvenients and the lack of standardisation thrust spirography with importants limitations when considering its use in a therapeutic trial or in the follow-up of a particular patient. Firstly, the necessity of that spiral specimens are always rated by the same assessor and secondly that postal assessments of patients, which have the potential advantage of providing a more realistic picture of the tremor severity (Bain et al., 1993), cannot be carried out. The analytical method developed by us is not conditioned by the above-described drawbacks. In particular, beside its objectivity and reproducibility, it is able to quantify any spiral drawing and it has not temporal or spatial limitations in the obtaining of spiral specimens.

Acknowledgements

This work was presented in part at the annual meeting of the Spanish Society of Neurology, Barcelona, Spain, November 2003. It constitutes part of the doctoral thesis of S.T. This study was funded in part by a grant of Conselleria de Sanitat i Consum. Govern de les Illes Balears.

Appendix A. Mathematical appendix

Since the co-ordinates (x, y), pertained to an Archimedean spiral, the following can be verified.

$$x = (-1)(r\ \cos(\alpha) + a_t\ \cos(\alpha_x)) \quad (1)$$

$$y = r\ \sin(\alpha) + a_t\ \sin(\alpha_y) \quad (2)$$

$$r = r_0 + \alpha\frac{K}{2\pi} \tag{3}$$

r_0 was the initial value of the spiral radius (r). α was the angle formed by (x, y) respect to x-axis. α changed from 0 to $n2\pi$; n was the number of spires ($n = 3$ in the present model). K was the increase in the spiral radius in each spire. The x co-ordinate was multiplied by -1 to make the spiral clockwise.

The terms $a_t \cos(\alpha_x)$ and $a_t \sin(\alpha_y)$ represent a periodic oscillation simulating a drawing tremor.

$$a_t = A\ \sin(\varpi \cdot t) \tag{4}$$

A was the maximal amplitude and ϖ was the frequency of tremor (in radians/s). 1 Hz is equal to 2π radians/s. If the oscillation had the same direction as the spiral radius, then $\alpha_x = \alpha_y = \alpha$. In the case that the oscillation was perpendicular to the x-axis, α_x and α_y had a constant value of $\pi/2$ radians.

The simulation was a numerical process that progressed through discrete increments of time ($\mathrm{d}t$). In the time t = zero, $x_0 = -1r_0$, y_0 = zero and $\alpha_0 = 0$ radians. From the known values of (x_0, y_0) and α_0, the values of (x, y) corresponding to the spiral co-ordinates at the time $t + \mathrm{d}t$ were calculated as follows. Firstly, the distance covered from (x_0, y_0) to (x, y) was

$$\mathrm{d}s = v\,\mathrm{d}t \tag{5}$$

v was the drawing velocity (in pixels/s). Secondly, a_t was calculated from the Eq. (4). Finally, α was increased from α_0 in the Eqs. (1)–(3) in discrete steps of $\mathrm{d}\alpha$ until a pair of co-ordinates (x, y) was found that verified

$$\mathrm{d}s = \sqrt{(x - x_0) + (y - y_0)^2} \tag{6}$$

The theoretical tremor spirals $\{(X_m, Y_m)\}$ were transformed and subsequently analysed by means of the FFT in the same way as experimental spirals.

The drawing velocity (v) was constant in some simulations while in others it was modelled according to the "two-thirds power law" (Lacquaniti et al., 1983)

$$v = g\kappa^{-\beta} \tag{7}$$

κ was the curvature of spiral (i.e. $1/r$) and β had the accepted value of 0.33 (Richardson and Flash, 2002). g is known as the gain factor; its value was found empirically by trial-and-error (see Section 3).

References

Alusi SH, Worthington J, Glickman S, Findley LJ, Bain PG. Evaluation of three different ways of assessing tremor in multiple sclerosis. J Neurol Neurosurg Psychiatry 2000;68:756–60.

Bain PG, Findley LJ, Atchinson P, Behari M, Vidailhet M, Gresty M, et al. Assessing tremor severity. J Neurol Neurosurg Psychiatry 1993;56:868–73.

Elble RJ, Sinha R, Higgins C. Quantification of tremor with a digitizing tablet. J Neurosci Methods 1990;32:193–8.

Elble RJ, Brilliant M, Leffler K, Higgins C. Quantification of essential tremor in writing and drawing. Mov Disord 1996;11:70–8.

Gonzalez RC, Woods RE. Digital image processing. 3rd ed. Reading, MA: Addison-Wesley; 1992.

Lacquaniti F, Terzuolo C, Viviani P. The law relating the kinematic and figural aspects of drawing movements. Acta Psychol 1983;54:115–30.

Liu X, Carroll CB, Wang X-Y, Zajicek J, Bain PG. Quantifying drug-induced dyskinesias in the arms using digitised spiral-drawing tasks. J Neurosci Methods 2005;144:47–52.

Longstaff MG, Mahant PR, Stacy MA, Van Gemmert AWA, Leis BC, Stelmach GE. Discrete and dynamic scaling of the size of continuous graphic movements of parkinsonian patients and elderly controls. J Neurol Neurosurg 2003;74:299–304.

Pullman SL. Spiral analysis: a new technique for measuring tremor with a digitizing tablet. Mov Disord 1998;13(Suppl. 3):85–9.

Richardson MJE, Flash T. Comparing smooth arm movements with the two-thirds power law and the related segmented-control hypothesis. J Neurosci 2002;22:8201–11.

Timmer J, Lauk M, Deuschl G. Quantitative analysis of tremor time series. Electroencephalogr Clin Neurophysiol 1996;101:461–8.